Kinetics of the Reactions of CH_3CH_2, CH_3CHCl, and CH_3CCl_2 Radicals with NO_2 in the Temperature Range 221−363 K

Matti P. Rissanen, Arkke J. Eskola,† Elena Savina, and Raimo S. Timonen*

Laboratory of Physical Chemistry, University of Helsinki, P.O. Box 55 (A.I. Virtasen aukio 1), FIN-00014 Finland

Received: October 17, 2008; Revised Manuscript Received: December 21, 2008

The gas-phase kinetics of three ethyl radical reactions with NO_2 have been studied in direct measurements using a laser photolysis/photoionization mass spectrometer (LP-PIMS) coupled to a temperature controlled tubular flow reactor. Reactions were studied under pseudo-first-order conditions with NO_2 always in large excess over initial radical concentrations. All the measured rate coefficients exhibit a negative temperature dependence, which becomes stronger as the chlorine substitution in the α-carbon of the ethyl radical increases. No pressure dependence of the rate coefficients was observed within the experimental range covered (0.5−6 Torr). The obtained results can be expressed conveniently as follows: $k(CH_3CH_2 + NO_2) = (4.33 \pm 0.13) \times 10^{-11}$ $(T/300\ K)^{-0.34 \pm 0.22}$ $cm^3\ s^{-1}$ (221−365 K), $k(CH_3CHCl + NO_2) = (2.38 \pm 0.10) \times 10^{-11}$ $(T/300\ K)^{-1.27 \pm 0.26}$ $cm^3\ s^{-1}$ (221−363 K), and $k(CH_3CCl_2 + NO_2) = (1.01 \pm 0.02) \times 10^{-11}$ $(T/300\ K)^{-1.65 \pm 0.19}$ $cm^3\ s^{-1}$ (248−363 K), where the given error limits are the 1σ statistical uncertainties of the plots of log k against log(T/300 K). Overall uncertainties in the measured rate coefficients were estimated to be ±20%. The observed reactivity toward NO_2 decreases with increasing chlorine substitution at the radical site as was expected with respect to our previous measurements of chlorine containing methyl radical reactions with NO_2. A potential reason for the observed reactivity differences is briefly discussed, and a possible reaction mechanism is presented.

Introduction

Chlorinated alkyl radicals are common intermediates in many combustion environments. They are ubiquitous in the incineration of hazardous wastes[1,2] and in industrial as well as other chlorination reactions of organic species.[3,4] They can increase soot formation in fuel-rich oxidation[5] and are connected with stratospheric ozone depletion.[6]

NO_2 is a pollutant emitted in large quantities from engine exhaust and almost all other combustion processes in the air. It is also one of the constituents of the natural unpolluted atmosphere.[7,8] NO_2 is a toxic substance and has an adverse impact on human health through the respiratory organs.[9,10] Enhanced NO_x production and a shifting of the balance from NO to NO_2 have been observed in a plasma treatment of halogenated pollutants.[11] The detailed information on the kinetics and reactivity of nitrogen oxides is needed for the modeling of the combustion processes because of their presence in almost all combustion environments and their intimate involvement in the processes.[12]

The chlorinated alkyl radicals (R) form weaker R−O_2 bonds than the corresponding nonchlorinated radicals. Therefore, the decompositions for the chlorinated peroxy radicals (R−O_2) are more probable than for the corresponding nonchlorinated peroxy radicals at combustion temperatures. As we compare the chlorinated and nonchlorinated radicals, the reactions for chlorinated radicals through alkyl radicals R are more probable than for nonchlorinated species, whereas nonchlorinated radicals react through a peroxy radical R−O_2 more probably than the chlorinated radicals.[13−16] This causes an accumulation of chlorine substituted alkyl radicals (compared to nonsubstituted radicals) under combustion conditions and a comparable increase in the likelihood of their reaction with species other than O_2.

Ethyl radicals (CH_3CH_2) are produced in hydrogen abstraction reactions from ethane by radicals (e.g., OH) and atoms (e.g., $O(^1D)$ or Cl) and, under elevated temperature conditions, by the unimolecular decomposition of larger hydrocarbons.[1,17] Photolysis of substituted ethanes, such as C_2H_5Br and C_2H_5I species, is also a possible source in the atmosphere.[18]

Chlorinated ethyl radicals (CH_3CHCl and CH_3CCl_2) are similarly formed in hydrogen abstraction reactions from ethyl chloride (CH_3CH_2Cl) and 1,1-dichloroethane (CH_3CCl_2H) by atoms and radicals. In these reactions, 1-chloroethyl radicals (CH_3CHCl) and 1,1-dichloroethyl radicals (CH_3CCl_2) are the most probable products because the α-C−H bonds are the weakest carbon−hydrogen bonds of ethyl chloride and 1,1-dichloroethane.[19,20]

In this paper we present results from direct time-resolved measurements of the rate coefficients of three radical reactions:

$$CH_3CH_2 + NO_2 \rightarrow \text{products} \quad (1)$$

$$CH_3CHCl + NO_2 \rightarrow \text{products} \quad (2)$$

$$CH_3CCl_2 + NO_2 \rightarrow \text{products} \quad (3)$$

To our knowledge, there are only two previous studies[21,22] of these reactions, both of which concern the $CH_3CH_2 + NO_2$ reaction. The first is a direct measurement by Park et al.,[21] ($k_{298K}(CH_3CH_2 + NO_2) = (4.5 \pm 0.9) \times 10^{-11}$ $cm^3\ s^{-1}$) at room temperature and low pressure using H-atom abstraction from ethane by chlorine atoms to produce the ethyl radicals and essentially the same technique for detection as is used in the present study. The second investigation is an indirect study by

* Corresponding author. E-mail:: raimo.timonen@helsinki.fi.
† Current address: School of Chemistry, University of Leeds, Leeds LS2 9JT, U.K.

10.1021/jp809193w CCC: $40.75
Published on Web 02/06/2009

Baulch et al.[22] at temperatures 298−363 K and about 300 Torr employing gas chromatography in the end product analysis of the $C_2H_6 + H_2O_2 + NO_2$ reaction mixtures.

To gain better understanding of the factors affecting chemical reactivity, it is valuable to study a series of reactions where only one parameter is changed at a time.[23] In the current work, this has been achieved by changing the Cl-substitution at the radical site.

Experimental Section

The experimental apparatus has been described in detail elsewhere,[24] and only an overview will be given here. The gas mixture flowing through the temperature controlled part of the tubular reactor contained the radical precursor (<0.5%), NO_2 (<0.5%), and an inert carrier gas (He) in large excess (>99%). The gas in the reactor was photolyzed along the axis of the reactor with an unfocused exciplex laser (ASX-750 or ELI-76) photolysis at 193 or 248 nm. The gas flow velocity was kept at about 5 m s^{-1} which ensured that the reactor was filled with a fresh gas mixture before the repetitive photolysis. The fluence of the photolyzing laser was measured outside of the reactor inlet before and after each experiment with a pyroelectric detector (Gentec ED-200) and was in the range 1−43 mJ cm^{-2} in a pulse. The reactor tubes used in measurements were made of seamless stainless steel with inner diameters of 8 and 17 mm and were coated with Halocarbon Wax (Supelco).

The gas mixture was continuously sampled through a small hole in the wall of the reactor and formed into a beam by a conical skimmer before entering the detection chamber. A portion of the gas beam was ionized with radiation from a resonance lamp, and the ions formed were mass-selected in a quadropole mass filter (Extrel, C-50/150-QC/19 mm rods). The mass-selected ion signals for the radicals and products were recorded with a multichannel scaler (EG&G Ortec MCS plus) from 15 ms before the laser pulse to about 80 ms after the photolysis. Typically, 2000−20000 laser pulses at a 5 Hz repetition rate were accumulated before an exponential function $\{[R]_t = [R]_0 \times \exp(-k't)\}$ was fit to the experimental data. In this equation $[R]_t$ is the signal proportional to the radical concentration at time t, and k' is the pseudo-first-order rate coefficient obtained from the fit to the decaying radical signal under given conditions.

The experiments were conducted under conditions where only two significant processes consumed the radical of interest: reaction with NO_2 and the heterogeneous loss on the walls of the reactor. In the beginning and at the end of measurements, the radical decay was measured without added reactant. The rate coefficient obtained in this way corresponds to all the other losses of the radical R in the system except for reactions with NO_2 and was termed the wall rate coefficient (k_{wall}). Initial radical concentrations were reduced until the wall loss rate did not depend on the reduction of laser fluence and/or precursor concentration and the first-order fit to the experimental data showed no noticeable deviation from first-order decay behavior.

After the wall rate measurement, NO_2 was added to the flow in varying amounts and the corresponding loss rates of the radical were measured for each NO_2 concentration. From the individual exponential fits to the first-order decaying radical signals the bimolecular rate coefficient of the studied reaction k_{R+NO_2} could be extracted by plotting the first-order rate coefficients k' against the NO_2 concentrations used: $k' = k_{wall} + k_{R+NO_2}[NO_2]$. A typical example is given in Figure 1 where a measurement of the $CH_3CHCl + NO_2$ reaction at 298 K and 6 Torr He is shown. The insets in the figure show the radical decay signal and the corresponding product formation signal. The amount of NO_2 was always in great excess over the radical concentration ($[NO_2] \gg [R]_0$) resulting in pseudo-first-order kinetics.

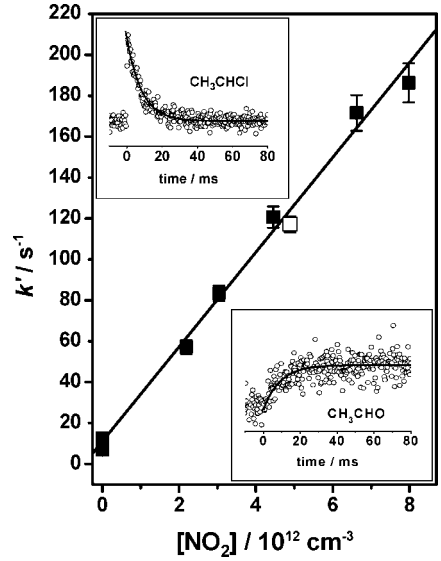

Figure 1. Plot of the pseudo-first-order rate coefficients as a function of reactant concentration used to obtain the bimolecular rate coefficient of the $CH_3CHCl + NO_2$ reaction under experimental conditions: T = 298 K and [He] = 1.95×10^{17} cm^{-3}. Shown in insets are, in the upper corner, the CH_3CHCl radical decay signal and, in the lower corner, the corresponding formation signal of the CH_3CHO product. The signals were measured under the conditions of the hollow square in the plot, where $[NO_2] = 4.89 \times 10^{12}$ cm^{-3}. The fitted lines in the insets are the first order decay and formation coefficients: $k'_d(CH_3CHCl) = (117 \pm 4)$ s^{-1} and k'_f $(CH_3CHO) = (111 \pm 10)$ s^{-1}. Uncertainties are one standard deviation (1Φ).

The handling of gaseous NO_2 in the experiments needs attention because its dimerization, if ignored, will cause an error in the calculated reactant concentration.[25] Also, NO_2 photolysis at the wavelengths used produces oxygen atoms in the reaction system. The absorption cross section of NO_2 is over 10 times larger at 193 nm ($\sigma_{193} = 2.9 \times 10^{-19}$ cm^{-2})[26] than at 248 nm ($\sigma_{248} = 1.62 \times 10^{-20}$ cm^{-2}),[18] and 193 nm photolysis produces excited singlet oxygen atoms $O(^1D)$ with a 55% yield.[26] This could cause problems in measuring the rate coefficients of the title reactions. Because of this, measurements were mainly performed at high precursor concentration and low laser intensity although some tests were made under the opposite conditions. Typical initial oxygen atom concentrations were in the range $(0.1-1) \times 10^{11}$ cm^{-3} and never exceeded 2×10^{11} cm^{-3}. Having tested many concentrations and laser intensities over a period of years, we have not seen any larger deviations than our uncertainties in the rate coefficients due to O-atoms.[27,28] The change of the laser intensity in the present work was more than a factor of 30, and no indication of O-atom interference in the results was observed. This shows that the isolation of the reactive species, at least up to a concentration of 5×10^{11} cm^{-3}, seems to be very good under the conditions of our measurements.

The decomposition of NO_2 dimer, N_2O_4, occurs very quickly when the NO_2 mixture expands from the gas bulb to the main gas flow. Under the conditions where reactant flow rates were measured (at about 6 Torr and 298 K), the unimolecular decomposition rate of N_2O_4 is about 1000

TABLE 1: Results and Conditions of the Experiments Used to Measure Reactions R + NO_2 → Products (R = CH_3CH_2, CH_3CHCl, and CH_3CCl_2)[a]

T/K	10^{-17}[He]/cm^{-3}	10^{-12}[NO_2]/cm^{-3}	$10^{12}k$/cm^3 s^{-1}	reactor i.d./mm	k_{wall}/s^{-1}
		R = CH_3CH_2 (CH_3CH_2 + NO_2 → Products)			
		$k(CH_3CH_2+NO_2) = (4.33 \pm 0.13) \times 10^{-12}$ (T/300 K)$^{-0.34\pm0.22}$ cm^3 s^{-1}			
221	1.33	1.18−4.36	50.2 ± 2.54	8[d]	19
241	1.78	1.13−5.74	43.0 ± 2.81	8[d]	48
254	1.29	1.16−5.80	48.8 ± 3.76	8[d]	17
267	1.66	1.15−5.79	44.5 ± 5.45	8[d]	57
298	0.19	0.94−2.29	40.6 ± 1.34	17[d]	3
298	0.45	1.19−4.78	43.2 ± 2.00	8[d]	14
298	1.29	1.08−5.45	49.3 ± 2.70	8[d]	21
298	1.55	1.31−6.22	35.6 ± 2.19	8[d]	47
298	1.63	2.31− 4.86	46.4 ± 1.41	8[d]	22
336	1.49	1.11−7.20	39.2 ± 3.32	8[d]	65
365	1.39	1.15−4.79	45.3 ± 2.22	8[d]	49
		R = CH_3CHCl (CH_3CHCl + NO_2 → Products)			
		$k(CH_3CHCl+NO_2) = (2.38 \pm 0.10) \times 10^{-11}$ (T/300 K)$^{-1.27\pm0.26}$ cm^{3}s^{-1}			
221	1.36	2.92−5.39	37.2 ± 4.21	8	50
241	1.29	4.80−10.1	28.5 ± 1.08	8	27
254	1.94	2.36−7.60	26.6 ± 0.79	8[b]	22
298	0.18	1.59−5.09	25.6 ± 1.17	17[b]	6
298	1.33	2.21−9.40	28.6 ± 2.45	8[c]	15
298	1.95	2.20−8.01	23.2 ± 0.90	8[b]	10
336	1.28	1.25−11.9	21.7 ± 0.52	8	25
363	1.27	1.32−12.5	16.4 ± 0.32	8	23
		R = CH_3CCl_2 (CH_3CCl_2 + NO_2 → Products)			
		$k(CH_3CCl_2 + NO_2) = (1.01 \pm 0.02) \times 10^{-11}$ (T/300 K)$^{-1.65\pm0.19}$ cm^3 s^{-1}			
248	0.65	2.40−10.5	12.9 ± 0.36	17	15
248	1.58	7.82−31.3	14.5 ± 0.39	8	34
266	0.65	2.34−8.95	13.0 ± 0.41	17	8
267	1.56	7.67−30.9	13.2 ± 0.67	8	20
282	1.37	2.48−12.5	12.1 ± 0.80	8	6
298	0.19	3.54−11.4	9.11 ± 0.45	17	4
298	0.65	7.10−15.1	9.22 ± 0.30	17[d]	1
298	0.68	6.22−15.5	10.1 ± 0.93	8	7
298	0.89	1.77−12.4	9.77 ± 0.95	17[d]	3
298	1.44	7.01−32.1	9.72 ± 0.33	8	13
298	1.95	6.10−17.0	10.8 ± 1.01	8	13
336	0.66	3.33−13.0	7.60 ± 0.62	17[d]	2
336	1.37	6.39−31.1	9.5 ± 0.62	8	7
363	0.65	4.69−13.2	6.98 ± 0.31	17[d]	1
363	1.36	6.74−33.1	8.19 ± 0.31	8	4

[a] Range of precursor concentrations used follows: (0.12−5.13) × 10^{14} cm^{-3} for CH_3CH_2Br, (1.17−2.90) × 10^{13} cm^{-3} for CH_3CHCl_2, (0.65−1.30) × 10^{13} cm^{-3} for $CH_3CHClBr$, and (0.24−6.02) × 10^{13} cm^{-3} for CH_3CCl_3. [b] Precursor CH_3CHCl_2. [c] 248 nm KrF-laser photolysis. [d] Estimated initial radical concentration was under 1 × 10^{11} cm^{-3}. In all the other experiments, the estimated initial radical concentration was under 8 × 10^{11} cm^{-3}. Statistical uncertainties shown are 1σ. Estimated overall uncertainty in the bimolecular rate coefficients is about ±20%.

s^{-1}.[25,29] This rapid dissociation rate together with the rather long residence time in the measuring volume ensures that almost all of the N_2O_4 is converted to NO_2 before the reactor inlet. That there may be a small amount of N_2O_4 in the reaction mixture does not interfere with the measured kinetics, because photolyzing N_2O_4 at the wavelengths used[18] produces only NO_2. Hence, it is only necessary to take into account the fraction of NO_2 that is in the form of N_2O_4 in the source bulb. This quantity can be calculated using equilibrium thermodynamics.[30] For the measurements, NO_2 was diluted in helium as 6−23% mixtures which correspond to 3−49% NO_2 as a dimer (N_2O_4) in the source bulb. The rate coefficients obtained with the different mixtures were the same within the experimental uncertainty, as can be seen in Table 1, for example for the CH_3CCl_2 + NO_2 reaction at temperatures T = 266 K and T = 267 K. The measurements were carried out with 23% and 15% mixtures of NO_2, respectively. The mixtures were stored and used in a blackened glass bulb to prevent the photochemical decomposition of NO_2.

The radicals of interest were produced in the photolysis of suitable precursors. The ethyl radicals were generated in the 193 nm photolysis of ethyl bromide. The primary dissociation channel is the C−Br bond fission:

$$CH_3CH_2Br + h\nu(193\text{ nm}) \rightarrow CH_3CH_2 + Br$$
$$\rightarrow \text{other products} \quad (4)$$

The dichloroethyl radicals were produced from methyl chloroform:

$$CH_3CCl_3 + h\nu(193\text{ nm}) \rightarrow CH_3CCl_2 + Cl$$
$$\rightarrow \text{other products} \quad (5)$$

Two different precursors, $CH_3CHClBr$ and CH_3CHCl_2, were used to produce the CH_3CHCl radical. One measurement was also made with 248 nm KrF-laser photolysis using $CH_3CHClBr$ as a radical source.

$$CH_3CHClBr + h\nu(193 \text{ or } 248\text{ nm}) \rightarrow CH_3CHCl + Br$$
$$\rightarrow \text{other products} \quad (6)$$

$$CH_3CHCl_2 + h\nu(193\ nm) \rightarrow CH_3CHCl + Cl$$
$$\rightarrow \text{other products} \quad (7)$$

Estimated initial radical concentrations were calculated from the absorption cross section,[18] concentration of the precursor, and laser intensity. If the absorption cross section was unavailable, the radical concentration was estimated on the basis of the precursor's decomposition signal and knowledge of the absorption spectrum for the same types of molecules. Initial radical concentrations were calculated to lie in the range (0.8−8) $\times 10^{11}$ cm^{-3} in all measurements. It was typically close to 1 $\times 10^{11}$ cm^{-3} but higher in the testing of possible interference from second order kinetics. The pressure changes in a fixed volume as a function of time were used to obtain the concentrations, and the pressure gauge used was a capacitance manometer (CCM instruments).

Several different products were sought with various ionization energies by changing the gas and the window material of the resonance lamp and by following the signal at the mass number for each probable product. The resonance lamps and energies used to ionize and detect the radicals and products in the present work were the following: a Cl-lamp with CaF_2 windows (8.9−9.1 eV) for CH_2CH, CH_3CH_2, CH_3CHCl, CH_3CCl_2, CCl_3, CH_2CCl_2, CH_2CCl_2, HCO, ClO, CH_3CO, CH_3CH_2O, CH_3CHClO; a H-lamp with MgF_2 windows (10.2 eV) for NO, NO_2, HNO, CH_3, C_2H_5, CH_3CHO, CH_3CH_2O, $CHCCl_2$, CH_2CCl, CH_2CCl_2, CH_2CHCl, CH_3CHCl, CH_3CCl_2, CH_3CCl_2O, CH_2CClO, CHClO, COCl, $COCl_2$, ClNO, $CH_3CHClNO_2$; and a Ne-lamp with a CHS (collimated hole structure) window (16.7 and 16.9 eV) for O, OH, H_2O, CO, Cl, Cl_2, ClO, COCl, CCl_2O, CHClO, CH_2CHCl, HCl, HCN, C_2H_4, CH_2O, CH_3OH, CH_3CClO, CH_3CCl_2O, CH_2CCl_2O, CH_3NO_2, $CH_3CH_2NO_2$, CH_2ClNO_2, $CH_3CHClNO_2$, $CH_3CCl_2NO_2$, CH_3CCl_2NO, CH_2CClNO, $ClNO_2$, NO_2, HNO_2, CH_2CO. For the title reactions, kinetic measurements were performed using the chlorine lamp; however, a few radical decay profiles were measured with a hydrogen lamp for comparison. When the hydrogen lamp was used for ionization instead of the chlorine lamp, the observed kinetics was unchanged. The only observable change was the greater intensity of the measured signal with the hydrogen lamp, due to the higher lamp intensity and probably more efficient ionization.

The radical precursors, ethyl bromide (CH_3CH_2Br, Aldrich, 98%), 1-bromo-1-chloroethane ($CH_3CHBrCl$, Alfa Aesar, 98%), 1,1-dichloroethane (CH_3CHCl_2, Aldrich, 97%), and 1,1,1-trichloroethane (CH_3CCl_3, Aldrich, 99%), were degassed prior to use by several freeze−pump−thaw cycles. Nitrogen dioxide gas (NO_2, Merck, 98%) was diluted in helium (He, Messer-Griesheim, 99.9996%) which was used as supplied.

Results and Discussion

The results of the current study together with the conditions of the measurements are presented in Table 1. No pressure dependence of the rate coefficients was observed within the experimental range covered (0.5−6 Torr) for any reactions. All the rate coefficients measured in this work exhibit a negative temperature dependence, which becomes stronger as the chlorine substitution at the radical site increases. Also, the reactivity of the radical toward NO_2 decreases with increasing substitution in the α-carbon, as can readily be seen in Figure 2 and Table 1. All of these observations were also made by Eskola et al.[27] for chlorinated methyl radicals in their study of the $CH_2Cl + NO_2$, $CHCl_2 + NO_2$, and $CCl_3 + NO_2$ reactions.

The only previous direct measurements of the title reactions have been performed by Park and Gutman.[21] They measured the bimolecular rate coefficient for the $C_2H_5 + NO_2$ reaction at $T =$ 298 K and 1−2 Torr pressure employing $Cl + C_2H_6 \rightarrow C_2H_5 +$ HCl reaction to produce the ethyl radicals and PIMS for detection. The obtained bimolecular rate coefficient $k_{298K}(CH_3CH_2 + NO_2) = (4.5 \pm 0.9) \times 10^{-11}$ cm^{3}s^{-1} is in excellent agreement with our current result $k_{300K}(CH_3CH_2 + NO_2) = (4.33 \pm 0.13) \times 10^{-11}$ cm^3 s^{-1}.

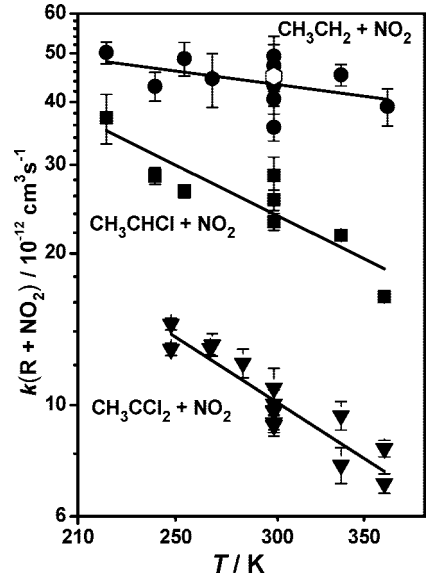

Figure 2. Double-logarithmic plots of the bimolecular reaction rate coefficients as a function of temperature measured in the current study. Included in the picture is also the rate coefficient of the $CH_3CH_2 + NO_2$ reaction measured by Park et al. [21] shown as a hollow hexagon. Uncertainties shown are one standard deviation (1σ).

All the $R + NO_2$ reaction rate coefficients obtained in the current study are notably higher than those for the corresponding O_2 reactions,[15,16,31] e.g., $k(CH_3CHCl + NO_2)/k(CH_3CHCl + O_2) \approx$ 13 under the conditions of the experiments. They could present a relatively small but significant loss process for the studied radicals under low temperature oxygen deficient combustion conditions.

Acetaldehyde was observed as a product of the $CH_3CHCl + NO_2$ reaction using a hydrogen lamp with a MgF_2 window for ionization. The CH_3CHO formation signal is presented in Figure 1 together with the corresponding CH_3CHCl radical decay signal. The decay rate equals the formation rate within the uncertainties of the rates given by the fits to the signals. This implies that acetaldehyde is the primary product of the $CH_3CHCl + NO_2$ reaction.

We could not observe any products for the $CH_3CH_2 + NO_2$ and $CH_3CCl_2 + NO_2$ reactions. On the basis of the previous experimental results on the $CH_3CH_2 + NO_2$ reaction,[21,22] we tried to search for nitroethane ($C_2H_5NO_2$, IE = 10.9 eV[17]) and ethyl nitrate (C_2H_5ONO, IE = 10.53 eV[17]) products but could not obtain any evidence for their formation. It was necessary to use a neon lamp with a CHS window (16.7 and 16.9 eV) for the ionization of these probable products, and that could have caused the fragmentation of these compounds. Detection of $C_2H_5NO_2$ could not be performed because the appearance energies for $C_2H_5^+$ and $C_2H_5O^+$ from nitroethane, $AE(C_2H_5^+ + NO_2) = 11$ eV and $AE(C_2H_5O^+ + NO) = 10.62$ eV, are much lower than the energy of the neon lamp.[17] Furthermore, using the Ne-lamp in ionization, our reactant ions and photodissociation fragments from the photoionization process are the same and so have the same mass numbers as our radical-ion R^+ and reactant NO_2. Park and Gutman[21] could identify nitroethane as a product from its principal fragment ion $C_2H_5^+$ due to a different experimental setup. They used a movable injector

and were able to follow the $C_2H_5^+$ signal (m/z = 29) under conditions where the CH_3CH_2 + NO_2 reaction is already fully completed, meaning the photodissociation of the product $CH_3CH_2NO_2$ in the photoionization. They were also able to use thin (0.1 mm, no longer available) LiF windows with an Ar-lamp to observe the completeness of the reaction. Detection of C_2H_5ONO was not possible for the same reasons as explained above. The appearance energy for the $C_2H_5O^+$ and NO products from ethyl nitrate is AE($C_2H_5O^+$ + NO) = 10.43.[17]

One experiment was conducted with 248 nm photolysis of $CH_3CHClBr$ as a CH_3CHCl radical source. The result of the measurement was consistent with those obtained at 193 nm photolysis although the radical signal quality was worse and resulted in larger than typical experimental uncertainties as can be seen in Figure 2 and Table 1. The estimated overall uncertainty in the reported bimolecular rate coefficients is about ± 20%. It originates mainly from the uncertainties in the calculated reactant concentrations and from the statistical uncertainties of fitting an exponential function to the radical signals. The impurities in the chemicals such as O_2 in He are minor sources of uncertainty. Due to the method used, the possible reactions of impurities, which do not photodecompose strongly in the laser pulse, will also be taken into account in the wall reaction (measurements with [NO_2] = 0) and therefore cancel out in the calculation of the reaction rate coefficients.

The possible impact of the heterogeneous processes on the walls of the reactor has been inspected in experiments (in this work) using different volume-to-surface area ratios by changing the diameter size of the reactor. Also, many combinations of the reactants and coverages of surfaces have already been tested previously under many conditions, and no larger effects than the uncertainties of our measurement results have been seen now or before.[27,28]

All the radical−radical reactions measured in this work are fast, lack pressure dependence, and exhibit negative temperature dependence. All of this suggests that the reactions proceed without any noticeable barrier in the entrance channel to form a collision complex either via O- or N-atom attack of NO_2 to the radical site. The possible further reactions of the formed complex depend on the energy of the system. The complex may form sets of bimolecular products, dissociate back to reagents, rearrange to various isomers, or stabilize in suitable conditions if the potential well for the molecular configuration is deep enough.

The mechanism of the studied reactions remains an interesting open question. There are no calculated potential energy surfaces available for these reactions. The observed product CH_3CHO in the CH_3CHCl + NO_2 reaction makes it tempting to suggest that the products could have been formed through a four center transition state (eq 8) which Sugawara et al.[32] have proposed for the CF_3 + NO_2 reaction to explain the formation of FNO and CF_2O products (here, the asterisk denotes internal excitation that can significantly change the observable end-products).

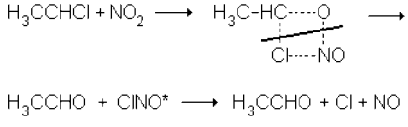

(8)

Alternatively, acetaldehyde could have been formed by a sequential fission of fragments through excited intermediates (eq 9) from the initial nitrite (R−ONO) adduct.

Kaiser et al.[33−35] and Orlando et al.[36] have studied the oxidation mechanism of ethyl chloride under atmospheric

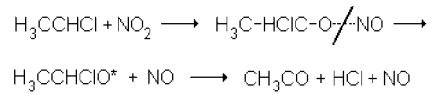

(9)

conditions and found that the CH_3CHClO radical produced will mainly undergo HCl elimination to form an acetyl radical (CH_3CO). Also, a theoretical study by Hou et al.[37] on the isomerization and decomposition of the CH_3CHClO species came to the same conclusion. The observed CH_3CHO product, previous direct and indirect studies on the CH_3CHClO radical decomposition, and the absence of a measurable CH_3CO signal support the suggested (eq 8) mechanism. Moreover, the observed acetaldehyde signal could not have been formed in a hydrogen abstraction reaction by CH_3CO, because it would be a secondary reaction and much too slow to account for the measured formation kinetics under the conditions of the experiments. Also, due to the background signals from the photolysis processes (a Cl atom which quickly produces HCl by abstracting hydrogen and an O atom that reacts with NO_2 to produce NO), the measured Cl and NO signals cannot be assigned with confidence to the primary products of the studied reactions. If nitrosyl chloride (ClNO, IE = 10.9 eV[17]) was produced in reaction (eq 8), it could not be detected for the same reasons as explained above for the NO_2-compounds; AE(NO^+ + Cl) = 11.0 eV.[17] It would be helpful in solving the problem if the formation of ClNO could be either detected or ruled out with a different experimental setup. We did not manage to detect any products for the CH_3CH_2 + NO_2 and CH_3CCl_2 + NO_2 reactions, and it is thus difficult to gain more insight into the underlying reaction mechanism(s).

Correlations between reactivity differences among radical reactions toward a common reagent (in the present case NO_2) and some readily obtainable radical properties have been sought in order to gain understanding of the factors affecting their chemical reactivity. One such example is the linear relationship of the electron affinity of the molecular reagent subtracted from the ionization potential of the radical plotted against the logarithm of the room temperature rate coefficient [(IP(R) − EA(reactant)) vs log(k_{300K})]. Paltenghi et al.[38] observed that this expression provides a good correlation for alkyl radical reactions with molecular oxygen and ozone. Another example is the Δelectronegativity scale, which is an arbitrary scale first proposed by Thomas[39] in another context and transmitted to radical kinetics by Gutman and co-workers.[40,41] It was discovered to be useful in explaining the observed differences in the rate coefficients of the methyl and halogenated methyl radical reactions with HI, and the same linear relationship was found to hold for larger alkyl radicals when an electronegativity value of 1.82 was assigned to the methyl group as a substituent. The purpose of the scale is to estimate the electron withdrawing inductive effect of the substituents as inferred from a simple sum of the Pauling electronegativities[42,43] of the substituent atoms/groups. It was shown to correlate linearly with the rate coefficients of the R + Cl_2[41] and R + Br_2[44] reactions. Both (IP(R) − EA(reactant)) vs log(k_{300K}) and Δelectronegativity versus log(k_{300K}) plots were also made for the reactions of the current study. Curiously, the (IP(R) − EA(reactant)) versus log(k_{300K}) relationship does not hold for NO_2 reactions with chlorinated alkyl radicals (Supporting Information Figures 1S and 2S); instead, the observed reaction rates correlate with EA(R) as was noted by Eskola et al.[27] The plots made are shown in Figure 3a,b together with selected previously measured data.

There exists a linear correlation of reactivity on both of the scales considered, especially among the studied ethyl radical

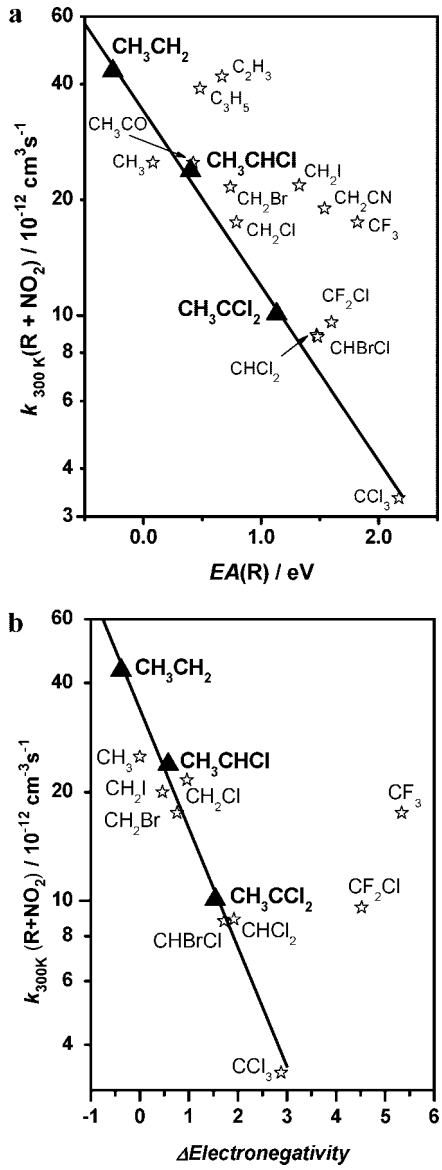

Figure 3. (a) Semilogarithmic plot of the measured bimolecular rate coefficients at room temperature versus the electron affinities of the radicals in the current and selected R + NO_2 reactions. The rate coefficient serves as a measure of the reactivity of the radical toward NO_2. Results from this study are presented as solid triangles. The line in the picture is a fit to the current results. The selected rate coefficients are from CH_2CN,[21] CH_2Cl, $CHCl_2$, CCl_3,[27] CH_2Br, CH_2I, CHBrCl,[28] C_2H_3, C_3H_5,[45] CH_3CO, CF_2Cl,[46] CH_3,[47] and CF_3.[48] Electron affinities were taken from ref 17 except for that of CH_2I, which is from ref 49, and for that of CHBrCl, which is from ref 50. In the case of substituted ethyl radicals, the EA of the radical was unavailable and was estimated with the help of ref 51, e.g., for CH_3CCl_2, $EA(CH_3CCl_2) = EA(CH_3CH_2) + (EA(CHCl_2) - EA(CH_3))$. (b) A semilogarithmic plot of the measured bimolecular rate coefficients at room temperature versus the Δelectronegativities of the radicals in the current and selected R + NO_2 reactions. Electronegativities were taken from Pauling,[42,43] and an electronegativity value of 1.82 was assigned to the methyl radical in accordance with ref 40. The line in the picture is a fit to the current results, which are shown as solid triangles. The selected rate coefficients are from CH_2Cl, $CHCl_2$, CCl_3,[27] CH_2Br, CH_2I, CHBrCl,[28] CF_2Cl,[46] CH_3,[47] and CF_3.[48]

reactions. This implies that polar effects, that is, charge density in the radical center, are likely to be important in determining the reactivity differences of the studied radicals in reactions with NO_2. In this case, the most polar species with the lowest charge density in the radical center (CH_3CCl_2) is the least reactive.

Conclusions

The bimolecular rate coefficients of the CH_3CH_2 + NO_2, CH_3CHCl + NO_2, and CH_3CCl_2 + NO_2 reactions have been measured in a direct time-resolved manner in the temperature range 221−363 K. The extent of chlorination is observed to significantly change the reactivity of the radicals toward NO_2. The only previous rate coefficient measurement of the studied reactions, at room temperature by Park and Gutman on the C_2H_5 + NO_2 reaction,[21] is in excellent agreement with our current results. All these reactions are fast and lack pressure dependence, and the rates increase with decreasing temperature. This suggests that the reactions are either barrierless or that the barrier is submerged below the energy of the separated reactants. The measured reactions are notably faster than the corresponding reactions with molecular oxygen and could present a certain loss process for these radicals under oxygen deficient, low temperature combustion conditions. A reaction mechanism, in which the formation of the R−NO_2* collision complex is followed by a four centered transition state leading to the observed products, has been suggested, and a probable cause for the observed reactivity difference is presented.

Acknowledgment. A.J.E. thanks the Finnish Cultural Foundation for the research grant. R.S.T. appreciates the support from the Bioscience and Environmental Research Council of the Academy of Finland and from the Maj and Tor Nessling Foundation.

Supporting Information Available: Selected room temperature rate coefficients of R + NO_2 reactions (k_{300K}) as a function of the ionization potential of the radical minus the electron affinity of the NO_2 Figures 1S and 2S. This material is available free of charge via the Internet at http://pubs.acs.org.

References and Notes

(1) Tsang, W. *Combust. Sci. Technol.* **1990**, *74*, 99.
(2) Cormier, S. A.; Lomnicki, S.; Backes, W.; Dellinger, B *Environ. Health Perspect.* **2006**, *114* (6), 810.
(3) Fettis, G. C.; Knox, J. H. In *Progress in Reaction Kinetics*; Porter, G., Ed.; MacMillen: New York, 1964; Vol. 2, pp 1−39.
(4) Poutsma, M. In *Methods in Free-Radical Chemistry*; Huyser, E. S., Ed.Marcel Dekker: New York, 1969; Vol. 1, pp 79−193.
(5) Violi, A.; D'Anna, A.; D'Alessio, A. *Chemosphere* **2001**, *42*, 463.
(6) *Scientific Assessment of Ozone Depletion 2006*; Global Ozone Research and Monitoring Project Report No. 50; WMO (World Meteorological Organization): Geneva, Switzerland, 2007; 572 pp.
(7) Wayne, R. P. *Chemistry of Atmospheres*, 3rd ed.; Oxford University Press, Inc.: New York, 2000; pp 164−480.
(8) Seinfeld, J. H.; Pandis, S. N. *Atmospheric Chemistry and Physics—From Air Pollution to Climate Change*; John Wiley & Sons, Inc.: New York, 1998; pp 67−74.
(9) Nitschke, M.; Smith, B. J.; Pilotto, L. S.; Pisaniello, D. L.; Abramson, M. J.; Ruffin, R. E. *Int. J. Environ. Health Res.* **1999**, *9*, 35.
(10) Mckee, D. J.; Rodriguez, R. M. *Water Air Soil Pollut.* **1993**, *67*, 11.
(11) Harling, A. M.; Whitehead, J. C.; Zhang, K. *J. Phys. Chem. A* **2005**, *109*, 11255.
(12) Miller, J. A.; Bowman, C. T. *Prog. Energy Combust. Sci.* **1989**, *15*, 287.
(13) Russell, J. J.; Seetula, J. A.; Gutman, D.; Danis, F.; Caralp, F.; Lightfoot, P. D.; Lesclaux, R.; Melius, C. F.; Senkan, S. M. *J. Phys. Chem.* **1990**, *94*, 3277.
(14) Knyazev, V. D.; Slagle, I. R. *J. Phys. Chem. A* **1998**, *102*, 1770.
(15) Knyazev, V. D.; Bencsura, A.; Dubinsky, I. A.; Gutman, D.; Melius, C. F.; Senkan, S. M. *J. Phys. Chem.* **1995**, *99*, 230.
(16) Knyazev, V. D.; Bencsura, A.; Slagle., I. R. *J. Phys. Chem. A* **1998**, *102*, 1760.
(17) Linstrom, P. J.; Mallard, W. G. *NIST Chemistry Webbook, NIST Standard Reference Database Number 69,* National Institute of Standards and Technology: Gaithersburg, MD, June, 2005; 20899; http://webbook.nist.gov.

(18) Sander, S. P.; Friedl, R. R.; Ravishankara, A. R.; Golden, D. M.; Kolb, C. E.; Kurylo, M. J.; Molina, M. J.; Moortgat, G. K.; Keller-Rudek, H.; Finlayson-Pitts, B. J.; Wine, P. H.; Huie, R. E.; Orkin, V. L. *Chemical Kinetics and Photochemical Data for Use in Stratospheric Modelling: Evaluation Number 15*; Publication 06-2; National Aeronautics and Space Administration, Jet Propulsion Laboratory, California Institute of Technology: Pasadena, CA, 2006.

(19) Niedzielski, J.; Tschuikow-Roux, E.; Yano, T *Int. J. Chem. Kinet.* **1984**, *16*, 621.

(20) Miyokawa, K.; Tschuikow-Roux, E. *J. Phys. Chem.* **1990**, *94*, 715.

(21) Park, J. Y.; Gutman, D. *J. Phys. Chem.* **1983**, *87*, 1844.

(22) Baulch, D. L.; Campbell, I. M.; Chappel, J. M. *J. Chem. Soc., Faraday, Trans. 1* **1984**, *80*, 599–628.

(23) Donahue, N. M. *Chem. Rev.* **2003**, *103*, 4593.

(24) Eskola, A. J.; Timonen, R. S. *Phys. Chem. Chem. Phys.* **2003**, *5*, 2557.

(25) Atkinson, R.; Baulch, D. L.; Cox, R. A.; Crowley, J. N.; Hampson, R. F.; Hynes, R. G.; Jenkin, M. E.; Rossi, M. J. Troe. *J. Atmos. Chem. Phys.* **2004**, *4*, 1461.

(26) Sun, F.; Glass, G. P.; Curl, R. F. *Chem. Phys. Lett.* **2001**, *337*, 72.

(27) Eskola, A. J.; Geppert, W. D.; Rissanen, M. P.; Timonen, R. S.; Halonen, L. *J. Phys. Chem. A* **2005**, *109*, 5376.

(28) Eskola, A. J.; Wojcik-Pastuszka, D.; Ratajczak, E.; Timonen, R. S. *J. Phys. Chem. A* **2006**, *110*, 12177.

(29) Borrell, P.; Cobos, C. J.; Luther, K. *J. Phys. Chem.* **1988**, *92*, 4377.

(30) Harwood, M. H.; Jones, R. L. *J. Geophys. Res.* **1994**, *99* (D11), 22955.

(31) Slagle, I. R.; Feng, Q.; Gutman, D. *J. Phys. Chem.* **1984**, *88*, 3648.

(32) Sugawara, K.; Nakanaga, T.; Takeo, H.; Matsumura, C. *J. Phys. Chem.* **1989**, *93*, 1894.

(33) Shi, J.; Wallington, T. J.; Kaiser, E. W. *J. Phys. Chem.* **1993**, *97*, 6184.

(34) Maricq, M. M.; Shi, J.; Szente, J. J.; Rimai, L.; Kaiser, E. W. *J. Phys. Chem.* **1993**, *97*, 9686.

(35) Kaiser, E. W.; Wallington, T. J. *J. Phys. Chem.* **1995**, *99*, 8669.

(36) Orlando, J. J.; Tyndall, G. S. *J. Phys. Chem. A* **2002**, *106*, 312.

(37) Hou, H.; Wang, B.; Gu, Y. *J. Phys. Chem. A* **2000**, *104*, 1570.

(38) Paltenghi, R.; Ogryzlo, E. A.; Bayes, K. D. *J. Phys. Chem.* **1984**, *88*, 2595.

(39) Thomas, T. D. *J. Am. Chem. Soc.* **1970**, *92*, 4184.

(40) Seetula, J. A.; Gutman, D. *J. Phys. Chem.* **1991**, *95*, 3626.

(41) Seetula, J. A.; Gutman, D.; Lightfoot, P. D.; Rayes, M. T.; Senkan, S. M. *J. Phys. Chem.* **1991**, *95*, 10688.

(42) Pauling, L. *Nature of the Chemical Bond,* 3rd ed; Cornell University Press: Ithaca, NY, 1960; pp 88−95..

(43) Allred, A. L. *J. Inorg. Nucl. Chem.* **1961**, *17*, 215.

(44) Timonen, R. S.; Seetula, J. A.; Niiranen, J.; Gutman, D. *J. Phys. Chem.* **1991**, *95*, 4009.

(45) Geppert, W. D.; Eskola, A. J.; Timonen, R. S.; Halonen, L. *J. Phys. Chem. A* **2004**, *108*, 4232.

(46) Slagle, I. R.; Gutman, D. *J. Am. Chem. Soc.* **1982**, *104*, 4741.

(47) Yamada, F.; Slagle, I. R.; Gutman, D. *Chem. Phys. Lett.* **1981**, *83*, 409.

(48) Breheny, C.; Hancock, G.; Morrell, C. *Phys. Chem. Chem. Phys.* **2000**, *2*, 5105.

(49) Born, M.; Ingemann, S.; Nibbering, N. M. M. *J. Am. Chem. Soc.* **1994**, *116*, 7210.

(50) Born, M.; Ingemann, S.; Nibbering, N. M. M *Int. J. Mass Spectrom. Ion Processes* **2000**, *194*, 103.

(51) Eskola, A. J. Ph.D. Thesis, University of Helsinki, Helsinki, 2007; http://urn.fi/URN:ISBN:978−952−10−3786−3.

JP809193W